



Article

Mapping Multi-Decadal Mangrove Extent in the Northern Coast of Vietnam Using Landsat Time-Series Data on Google Earth Engine Platform

Thuy Thi Phuong Vu ¹, Tien Dat Pham ^{2,*} , Neil Saintilan ², Andrew Skidmore ^{2,3} , Hung Viet Luu ⁴, Quang Hien Vu ¹, Nga Nhu Le ⁵ , Huu Quang Nguyen ⁶ and Bunkei Matsushita ⁷

- ¹ Forest Inventory and Planning Institute (FIPI), Ministry of Agricultural and Rural Development (MARD), Vinh Quynh, Thanh Tri, Hanoi 100000, Vietnam
 - ² School of Natural Sciences, Faculty of Science and Engineering, Macquarie University, Sydney, NSW 2109, Australia
 - ³ Faculty of Geo-Information Science and Earth Observation (ITC), University of Twente, 7522 NB Enschede, The Netherlands
 - ⁴ Centre of Multidisciplinary Integrated Technologies for Field Monitoring (FIMO), The University of Engineering and Technology, Vietnam National University (VNU), 144 Xuan Thuy, Cau Giay, Hanoi 100000, Vietnam
 - ⁵ Department of Marine Mechanics and Environment, Institute of Mechanics, Vietnam Academy of Science and Technology (VAST), 264 Doi Can Street, Ba Dinh District, Hanoi 100000, Vietnam
 - ⁶ Department of Policy and Planning Sciences, University of Tsukuba, 1-1-1 Tennoudai, Tsukuba 305-8573, Ibaraki Prefecture, Japan
 - ⁷ Faculty of Life and Environmental Sciences, University of Tsukuba, 1-1-1 Tennoudai, Tsukuba 305-8572, Ibaraki Prefecture, Japan
- * Correspondence: tiendat.pham@mq.edu.au



Citation: Vu, T.T.P.; Pham, T.D.; Saintilan, N.; Skidmore, A.; Luu, H.V.; Vu, Q.H.; Le, N.N.; Nguyen, H.Q.; Matsushita, B. Mapping Multi-Decadal Mangrove Extent in the Northern Coast of Vietnam Using Landsat Time-Series Data on Google Earth Engine Platform. *Remote Sens.* **2022**, *14*, 4664. <https://doi.org/10.3390/rs14184664>

Academic Editor: Guangsheng Chen

Received: 22 July 2022

Accepted: 16 September 2022

Published: 19 September 2022

Publisher's Note: MDPI stays neutral with regard to jurisdictional claims in published maps and institutional affiliations.



Copyright: © 2022 by the authors. Licensee MDPI, Basel, Switzerland. This article is an open access article distributed under the terms and conditions of the Creative Commons Attribution (CC BY) license (<https://creativecommons.org/licenses/by/4.0/>).

Abstract: A pixel-based algorithm for multi-temporal Landsat (TM/ETM+/OLI/OLI-2) imagery between 1990 and 2022 monitored mangrove dynamics and detected their changes in the three provinces (i.e., Thai Binh, Nam Dinh and Hai Phong), which are located on the Northern coast of Vietnam, through the Google Earth Engine (GEE) cloud computing platform. Results showed that the mangrove area in the study area decreased from 2960 ha in 1990 to 2408 ha in 1995 and then significantly increased to 4435 ha in 2000 but later declined to 3502 ha in 2005. The mangrove areas experienced an increase from 4706 ha in 2010 to 10,125 ha in 2020 and reached a highest peak of 10,630 ha in 2022. In 2022, Hai Phong province had the largest area of mangrove (3934 ha), followed by Nam Dinh (3501 ha) and Thai Binh (3195 ha) provinces. The overall accuracies for 2020 and 2022 were 94.94% and 91.98%, while the Kappa coefficients were 0.90 and 0.84, respectively. The mangrove restoration programs and policies by the Vietnamese government and local governments are the key drivers of this increase in mangroves in the three provinces from 1990 to 2022. The results also demonstrated that the combination of Landsat time series images, a pixel-based algorithm, and the GEE platform has a high potential for monitoring long-term change of mangrove forests during 32 years in the tropics. Moreover, the obtained mangrove forest maps at a 30-m spatial resolution can serve as a useful and up-to-date dataset for sustainable management and conservation of these mangrove forests in the Red River Delta, Vietnam.

Keywords: mangrove; remote sensing; Landsat; Google Earth Engine; Red River Delta; Vietnam

1. Introduction

Mangrove forests are trees and shrubs found in tidal wetlands and located in the tropical and sub-tropical region between 30°N and 30°S latitude [1]. They cover only 0.1% of Earth's continental surface, yet they provide a wide range of ecosystem services, including water purification, natural hazards reduction, soil and water conservation, shoreline

protection and enhanced local livelihood and are considered as natural-based solutions in dealing with climate change impact [2]. The areas of mangrove forests have been changed significantly on a global scale due to anthropogenic disturbance (i.e., urbanization and increased agricultural production) and climate change [2]. However, recent studies pointed out that the rate of deforestation has been decreasing [3], and mangroves have expanded in some Southeast Asian nations and in Australia [4,5].

Among approximately 3260 km of the total coastal length of Vietnam, 2365 km are covered by mangroves representing 29 coastal provinces. Mangrove ecosystems, therefore, play an important role in protecting the Vietnamese coastline against flooding and erosion, providing biodiversity and livelihood for coastal communities as well as sequestering carbon, known as 'blue carbon' [6,7]. The Vietnamese mangroves are mainly distributed in the two deltas, the Red River Delta (RRD) in the north and the Mekong River Delta in the south [8,9]. However, the mangrove forest area in Vietnam has decreased dramatically over the past 70 years, falling from 408,500 ha in 1943 to 178,000 ha in 2000, and then continuously shrinking to 138,318 ha in 2016 [10–14]. Therefore, it is essential to obtain accurate information about mangrove forests in the past and current state that is useful to manage and effectively protect mangrove ecosystems across the Vietnamese coastline. However, there is no up-to-date map of mangroves in Vietnam; thus, mapping mangrove forests and detecting their dynamics are vital for sustainable conservation and management of mangrove resources.

Mapping mangroves at a large scale remains challenging due to the costs and labour intensiveness in field measurements for large areas. In recent years, remote-sensing-based techniques have become widely used for monitoring the Earth's surface including mangrove forests and has proven to be a key tool to effectively map mangrove dynamics in large areas in Southeast Asia [12,15–18]. Pixel-based and object-based approaches are the most common techniques for mapping mangroves and detecting their changes. These approaches can provide the most frequently updated data at a low cost [19,20]. For instance, the distribution of mangroves at a global scale using a multi-temporal Landsat dataset and a supervised Maximum Likelihood Classification (MLC) was reported by Giri et al. [17] with an overall accuracy ranging from 79% to 86%. In Vietnam, Nguyen-Thanh et al. [12] used the Landsat time series data and an object-based image analysis to monitor mangrove extent in the Ca Mau Peninsula, Vietnam, whereas Pham and Brabyn [13] used the SPOT imagery and a support vector machine (SVM) classifier to map mangrove dynamics in the Can Gio biosphere reserve region with overall accuracies of 77 and 83%. However, to date there is no spatial distribution map of mangroves along the RRD, and there is a complete lack of reliable updated statistical data of mangroves in the three coastal provinces of the RRD.

More recently, with the development of open-source software and cloud computing platforms such as the Google Earth Engine (GEE), the applications of remote sensing techniques in monitoring mangrove changes have become more popular. Previous studies have widely applied the GEE platform to map mangrove changes using multispectral sensors such as the Thematic Mapper (TM), the Enhanced Thematic Mapper Plus (ETM+), the Operational Land Imager (OLI), and the Operational Land Imager-2 (OLI-2) in Landsat and the Multi-Spectral Instrument (MSI) in Sentinel-2 [21–25]. However, to the best of our knowledge, the up-to-date mangrove forests maps and their change detection using time series Landsat (TM/ETM+/OLI/OLI-2) imagery between 1990 and 2022 have not been reported in Vietnam. Thus, this study aims to fill the gap in the current literature by investigating a pixel-based algorithm: (1) to map multi-decadal mangrove dynamics using Landsat time series data between 1990 and 2022 through the GEE platform, (2) to provide up-to-date statistical analysis of areas of mangrove forests in the Northern coast of Vietnam for the first time in 2022 using Landsat-9 OLI-2 as an important national mangrove database, and (3) to provide a useful tool for decision makers in supporting the mangrove conservation and management in Vietnam.

2. Materials and Methods

2.1. Study Area

In the current study, three coastal provinces in the RRD were selected to test the performance of the pixel-based algorithm. They are Hai Phong province ($20^{\circ}51'54.5004''\text{N}$, $106^{\circ}41'1.7880''\text{E}$), Thai Binh province ($20^{\circ}27'0''\text{N}$, $106^{\circ}20'24.07''\text{E}$) and Nam Dinh province ($20^{\circ}16'45.048''\text{N}$, $106^{\circ}12'18.533''\text{E}$), which are shown in Figure 1.

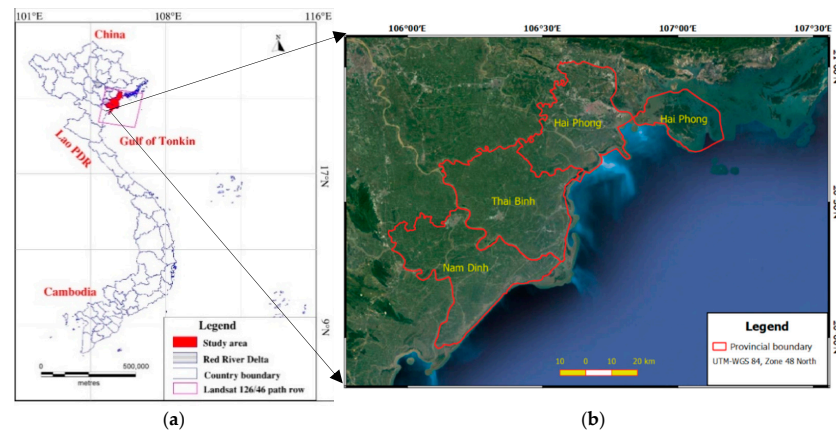


Figure 1. Study area in the northern coast of Vietnam: (a) map of Vietnam; (b) three coastal provinces in the RRD.

The RRD, consisting of nine provinces (i.e., Hai Duong, Bac Ninh, Vinh Phuc, Hung Yen, Thai Binh, Nam Dinh, Ha Nam, Ninh Binh and Quang Ninh) is the second-largest delta and is located in the northern region of Vietnam with a total area of 15,000 km². With a population of 22 million, the RRD is the most densely populated region in Vietnam [26]. In 2019, the population density of the RRD had reached 1064 inhabitants per km² [27]. The total area of the three provinces is approximately 473,700 ha, of which Nam Dinh province is the largest with 166,800 ha, followed by Thai Binh province and Hai Phong province with an area of 153,400 ha and 152,300 ha, respectively [8].

The mangrove ecosystems in the RRD play a key role in protecting coastal habitats, supporting biodiversity, and providing coastal resources for local people. In the RRD, the Xuan Thuy National Park was listed as the first Ramsar site in Southeast Asia in 1989 to promote the sustainable conservation of wetlands [28]. The Ramsar site was defined as “the sustainable utilization of wetlands for the benefit of mankind in a way compatible with the maintenance of the natural properties of the ecosystem” [29]. There are five dominant mangrove species observed in this park being *Sonneratia caseolaris*, *Kandelia obovata*, *Aegiceras corniculatum*, *Rhizophora stylosa* and *Avicennia marina* [30]. Furthermore, this park is the habitat to 116 flora species and 106 fish and has significantly contributed to wetland biodiversity protection on the northern coastline of Vietnam [30]. A nature reserve, which is located in Thai Binh Province, is well-known as the Bird Conservation area, and there are several rare species listed in the Vietnamese Red Book [27]. There are four seasons in the RRD with a mean annual temperature of approximately 28 °C. The annual precipitation recorded in the last ten years is around 1800–2000 mm. In recent years, the RRD has been seriously affected by climate variability including higher temperatures, storms and flooding [28]. In particular, 2020 was recorded as the hottest year over the last 45 years and likely resulted in a dieback of mangroves [31,32].

2.2. Materials

Satellite Data

Multi-decadal Landsat surface reflectance (SR) data obtained through the GEE platform was used to map mangrove dynamics in the study area (Table 1). We used Collection 2, which were atmospherically corrected SR data with a single-channel algorithm developed

by the National Aeronautics and Space Administration (NASA) Jet Propulsion Laboratory (JPL). All Landsat time series Collection 2 SR data used in the current study (Table 1) were acquired using the Java scripts on the GEE.

Table 1. Time-series Landsat imagery used for 32 years in the study area.

Sensor	Spatial Resolution (m)	Path/Row	Year	Band Used
Landsat-5 TM	30	126/46	1990, 1995, 2005, 2010	Blue, Green, Red, NIR, SWIR
Landsat-7 ETM+	30	126/46	2000	
Landsat-8 OLI	30	126/46	2015, 2020	
Landsat-9 OLI-2	30	126/26	2022	

Considering the seasonality changes of mangrove forests and their species, a total of 82 cloud-free Landsat scenes between 1990 and 2022 were used to map mangrove dynamics in the RRD. We applied an image normalisation technique to make all images consistent during the pre-processing process. To minimize the effects of tidal and water levels, we selected the datasets acquired in early morning when the tidal level was the lowest.

2.3. Methods

2.3.1. Generation of Training and Validation Datasets for the Study Area

In this study, the training and the validation data were obtained from very high spatial resolution images in Google Earth Pro imagery (2020). A total of 2370 points were randomly selected, of which 1896 points (80%) were used for the training set and 474 points (20%) were used for the validation set (Figure 2).

As shown in Figure 2, a polygon including mangrove forest and non-mangrove was created from the spatial data and consisted of a sea dyke and river layers with a total area of 35,566 ha. A 3 km buffer generated from the high-resolution images of Google Earth Pro imagery in 2020 was used to capture the entire mangrove forests area as suggested by Thomas et al. [33] and Bunting et al. [34].

2.3.2. Computation of Spectral Indices

Four indices were calculated from the SR data of Landsat (5/7/8/9) images to identify vegetation and open surface water bodies as suggested by Wang et al. [22] and Pham et al. [35]. They are the Normalized Difference Vegetation Index (NDVI) [36], the Enhanced Vegetation Index (EVI) [37], the Land Surface Water Index (LSWI) [38] and the modified Normalized Difference Water Index (mNDWI) [39]. The equations are shown below:

$$\text{NDVI} = \frac{\rho_{nir} - \rho_{red}}{\rho_{nir} + \rho_{red}} \quad (1)$$

$$\text{EVI} = 2.5 \times \frac{\rho_{nir} - \rho_{red}}{\rho_{nir} + 6 \times \rho_{red} - 7.5 \times \rho_{blue} + 1} \quad (2)$$

$$\text{LSWI} = \frac{\rho_{nir} - \rho_{swir}}{\rho_{nir} + \rho_{swir}} \quad (3)$$

$$\text{mNDWI} = \frac{\rho_{green} - \rho_{swir}}{\rho_{green} + \rho_{swir}} \quad (4)$$

where ρ_{red} , ρ_{green} , ρ_{blue} and ρ_{swir} are the surface reflectance at red (band 3 for TM/ETM+ or band 4 for OLI and OLI-2), green (TM/ETM+ band 2 or OLI/OLI-2 band 3), blue (TM/ETM+ band 1 or OLI/OLI-2 band 2) and short-wave infrared (SWIR: TM/ETM+ band 5 or OLI/OLI-2 band 6) bands, respectively.

We proposed a framework using a pixel-based mapping algorithm to map mangrove forests and automatically detect their changes using time series Landsat images from 1990 to 2022 through the GEE platform as shown in Figure 3. We developed the Python scripts using the geemap package (<https://github.com/giswqs/geemap>, accessed on 16 July 2021) to map mangrove extent in the RRD.

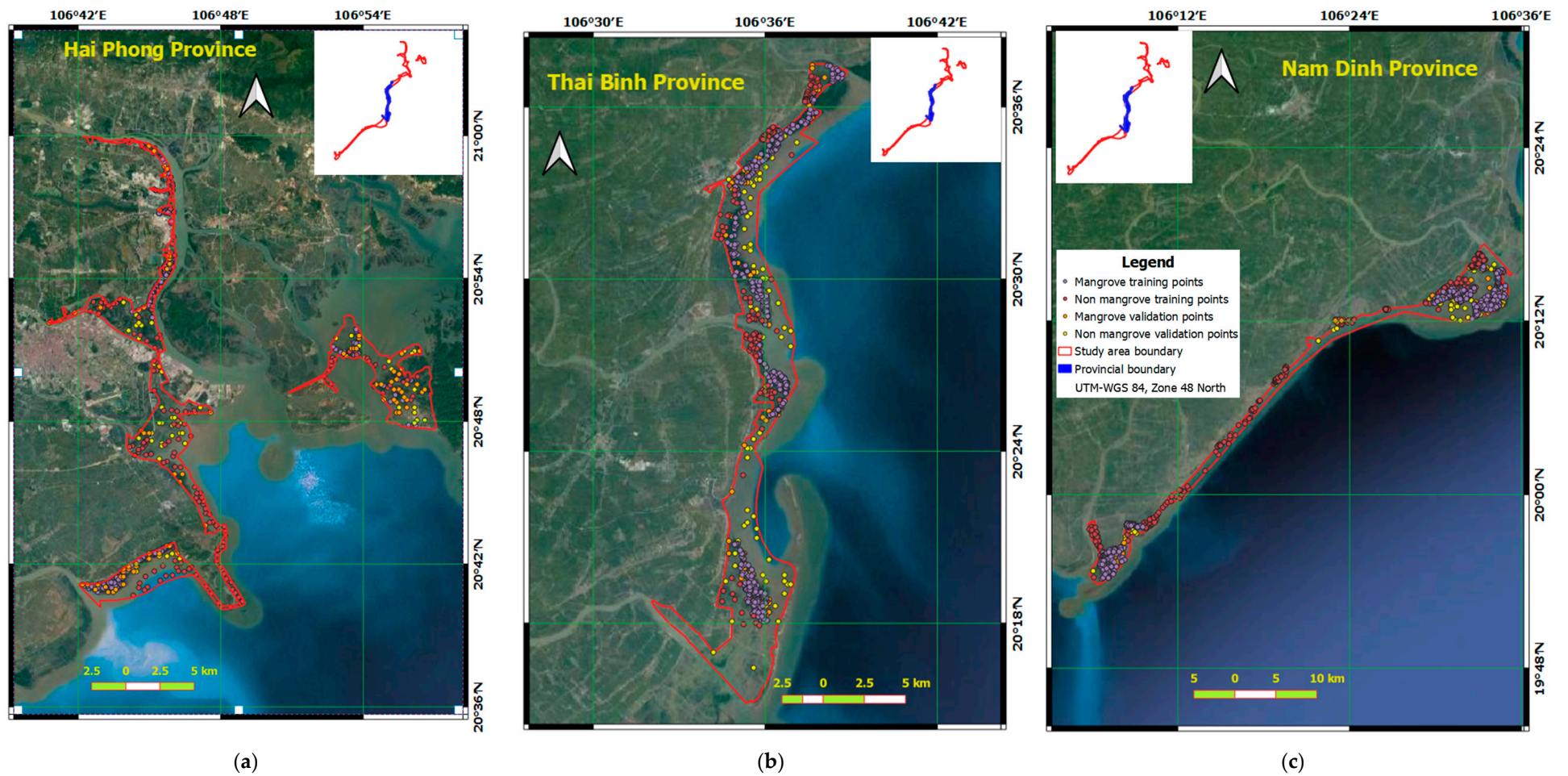


Figure 2. Training and validation points for mangrove mapping during the year 2020 in the RRD, Vietnam: (a) Hai Phong; (b) Thai Binh; (c) Nam Dinh.

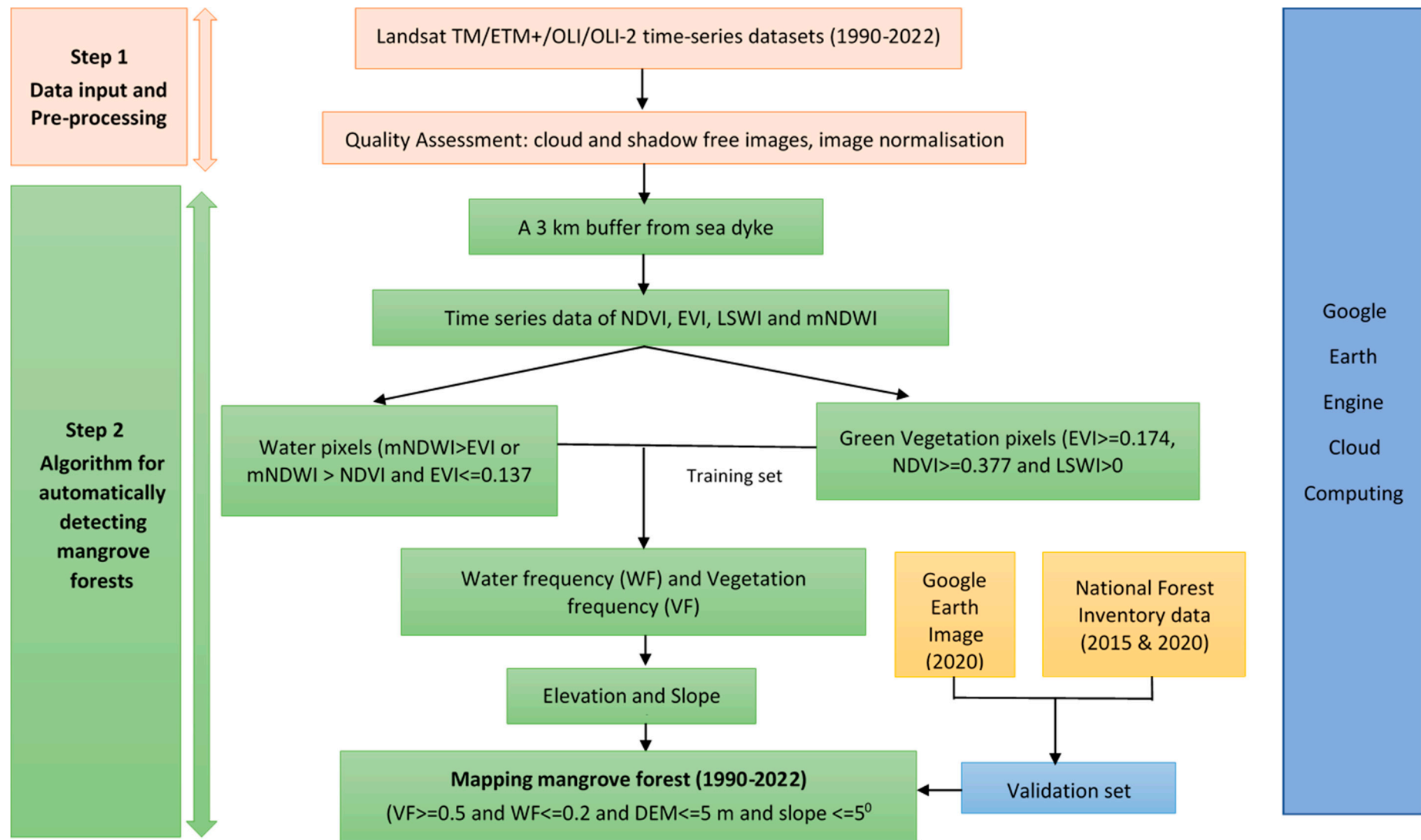


Figure 3. A framework developed in this study for mangrove mapping and change detection using a pixel-based algorithm.

2.3.3. Mangrove Mapping Algorithm

In this study, we used a pixel-based algorithm, which was developed by Wang et al. [22] for mapping coastal wetlands using time series Landsat datasets in 2018 to generate annual maps of mangrove forests between 1990 and 2022. The algorithm includes three steps for processing each pixel: (1) identifying open surface water body and green vegetation, (2) calculating annual frequency for surface water body and vegetation, and (3) generating annual maps of mangrove forest. The present study used data in 2020 and in 2022 to check and modify the thresholds provided by the original study and then used these modified thresholds to estimate the mangrove area for other years.

We used a frequency-based approach from Landsat time series to mitigate the effect of periodical tidal dynamics and bad-quality observations as suggested by Wang et al. [22]. The open surface water body and vegetation frequencies in a year were calculated using the following equations:

$$WF = \frac{N_{\text{water}}}{N_{\text{good}}} \quad (5)$$

$$VF = \frac{N_{\text{vegetation}}}{N_{\text{good}}} \quad (6)$$

where

WF and VF are the frequencies of surface water body and vegetation, respectively (−1 to 1).

N_{water} and $N_{\text{vegetation}}$ are the numbers observations identified as water and vegetation in a year, respectively, while

N_{good} is the number of observations with good quality, which was characterised as cloud and shadow-free during the observed year.

We defined the thresholds based on the training data collected from the high spatial resolution Google Earth images in 2020 to identify evergreen wetlands as follows:

$$\text{Evergreen} = VF \geq 0.9 \text{ and } WF \leq 0.2 \text{ and } \text{DEM} \leq 5 \text{ m and } \text{Slope} \leq 5^\circ \quad (7)$$

where WF and VF are the frequencies of surface water body and vegetation, respectively. These indices values are ranked between −1 and 1, while the Shuttle Radar Topography Mission (SRTM) Digital Elevation Model (DEM) data were used to generate a slope layer in the current study [22].

To identify open surface water bodies and green vegetation, a combination of mNDWI and two vegetation indices (EVI and NDVI) was employed to reduce the errors in mixed pixels of the water body and vegetation [22]. In this study, almost all pixels identified as water body in 2020 have an $EVI \leq 0.137$ and $mNDWI > EVI$ or $mNDWI > NDVI$.

The NDVI and the EVI are two popular indices to detect vegetation as suggested in prior studies [19,27]. Their values are defined between −1 to 1 in which the negative values indicate no vegetation, while greater positive values indicate available green vegetation cover. However, a given pixel is often mixed on vegetation, water and soil. The LSWI is an alternative useful index to identify water content in vegetation and soil, and its values are also between −1 to 1. The current study found that most vegetation pixels have $EVI \geq 0.174$, $NDVI \geq 0.377$ and $LSWI \geq 0$. The final formulations to identify surface water body and green vegetation in 2020 are shown as below:

- Pixels of surface water body: $EVI \leq 0.137$ and ($mNDWI > EVI$ or $mNDWI > NDVI$);
- Pixels of green vegetation: $EVI \geq 0.174$, $NDVI \geq 0.377$ and $LSWI > 0$.

2.3.4. Annual Maps of Mangrove Forest

As shown in Figure 3, almost all vegetation pixels have values of $VF \geq 0.5$, while water pixels have WF values ranging from 0.05 to 0.85. In addition, both mangrove and

non-mangrove pixels have $DEM \leq 5$ m and $Slope \leq 5^\circ$. Therefore, the criteria for mangrove mapping in 2020 and in 2022 was described as follows:

$$\text{Mangrove forest} = VF \geq 0.5 \text{ and } WF \leq 0.2 \text{ and } DEM \leq 5 \text{ m and } Slope \leq 5^\circ \quad (8)$$

$$\text{Non-mangrove forest} = VF \leq 0.15 \text{ and } 0.05 \leq WF \leq 0.2 \text{ and } DEM \leq 5 \text{ m and } Slope \leq 5^\circ \quad (9)$$

2.3.5. Accuracy Assessment

The mangrove maps of the three provinces in 2020 and in 2022 were generated from Landsat-8 OLI and Landsat-9 OLI-2 data using the modified algorithm through the GEE cloud computing platform. In this study, the stratified random sampling approach was employed to generate the verification samples, and very high-resolution images were used to evaluate the accuracy of the classification maps in 2020 and in 2022. The size of verification points for each class (mangrove or non-mangrove) was identified by Cochran's formula (the confidence level was set to 0.95 in this study):

$$n_0 = \frac{Z^2 pq}{e^2} \quad (10)$$

where

n_0 is the sample size,

Z is derived from the standard normal distribution,

e is the desired level of precision,

p is the required accuracy, and

$q = 1 - p$.

In this study, a total of 474 validation points (20% of the total points) were selected for evaluating the accuracy of mangrove forest mapping in 2020 and in 2022. The random sampling points include 243 mangrove samples and 231 non-mangrove samples. Then, each sample was checked with its location, which was identified from very high spatial resolution Google Earth images by visual interpretation. With the validation samples, the user's accuracy, the producer's accuracy, the overall accuracy, and the Kappa coefficient were calculated in this study [35,40].

2.3.6. Analysis and Statistical Method

The mangrove distribution maps and the mangrove statistical areas in the study sites were automatically computed. In addition, the present study used QGIS 3.10.2 software to produce the spatial distribution of mangroves in the RRD of Vietnam.

3. Results

3.1. Mangrove Classification and Accuracy Assessment

As shown in Figure 4, the total area of mangrove forest was estimated as 10,125 ha and 10,630 ha in 2020 and in 2022, respectively. The largest mangrove forest area was observed in Hai Phong province (3790 ha), followed by Nam Dinh province (3325 ha) and Thai Binh province (3010 ha) in 2020.

The results in Tables 2 and 3 show that the overall accuracies obtained from the stratified random sampling points were 94.94% in 2020 and 91.98% in 2022, while the Kappa coefficients of classification maps for 2020 and 2022 were 0.90 and 0.84, respectively, indicating a good-of-fit agreement between the classification result and reference data. The Landsat-8 OLI sensor produced relatively higher accuracy for 2020 than that of the Landsat-9 OLI-2 sensors for 2022.

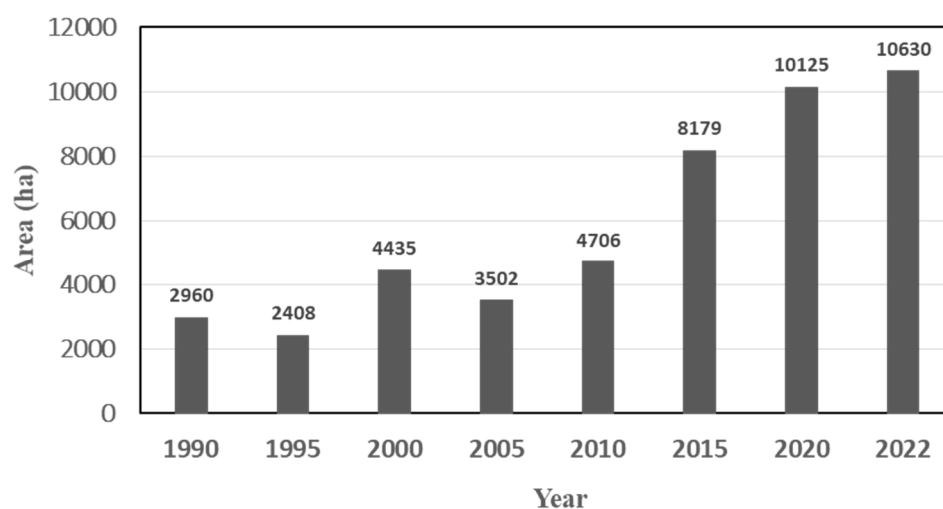


Figure 4. The estimated mangrove area in the RRD from 1990 to 2022.

Table 2. The confusion matrix for accuracy assessment of mangrove forest using Landsat 8-OLI in 2020.

		Reference Pixels			User's accuracy	
		Class	Mangrove	Non-mangrove		Total
Predicted pixels	Mangrove		221	22	243	90.95%
	Non-mangrove		2	229	231	99.13%
	Total		223	251	474	
	Producer's Accuracy		99.10%	88.18%		
	Overall accuracy		94.94%			
	Kappa coefficient		0.90			

Table 3. The confusion matrix for accuracy assessment of mangrove forest using Landsat-9 OLI-2 in 2022.

		Reference Pixels			User's accuracy	
		Class	Mangrove	Non-mangrove		Total
Predicted pixels	Mangrove		210	33	243	86.42%
	Non-mangrove		5	226	231	97.84%
	Total		215	259	474	
	Producer's Accuracy		97.70%	87.26%		
	Overall accuracy		91.98%			
	Kappa coefficient		0.84			

3.2. Mangrove Dynamics from 1990 to 2022

By using our defined thresholds in 2020 and the proposed framework in Figure 3, we generated mangrove maps in the three provinces (Hai Phong, Nam Dinh and Thai Binh) in the RRD between 1990 and 2015 together with mangrove maps in 2022 (See Figures A1–A3). We also estimated the areas of mangrove forests in the three provinces for other years (1990, 1995, 2000, 2005, 2010, 2015 and 2022). The mangrove distribution maps and the statistical areas in the study sites were automatically computed using the Java scripts on the GEE cloud computing platform. As shown in Figure 4, the mangrove forest area increased in the three provinces across the RRD over the 32 years (1990–2022). The change of mangrove area in each province and each period can be found in Table 4. Figure 5 shows the spatial distribution of mangrove in the RRD of Vietnam in 1990 (Figure 5a) and in 2022 (Figure 5b). Figures 6 and 7 represent the mangrove maps of each province in the RRD in 1990 (Figure 6)

and in 2022 (Figure 7). Mangrove forests are mainly distributed in the river mouth of the three provinces in the RRD, and they are found in front of the sea dykes (Figures 5–7).

As shown in Figure 4, the area of mangrove forests in the RRD significantly increased from 1990 to 2022. The mangrove area decreased from 2960 ha in 1990 to 2408 ha in 1995 and then significantly increased to 4435 ha in 2000. Notably, the area of mangrove forests decreased to 3502 ha in 2005. In contrast, the mangrove area experienced an increase from 4706 ha in 2010 to 8179 ha in 2015 and continued its upward trend to 10,125 ha in 2020 and reached the highest peak value of 10,630 ha in 2022.

Table 4 shows the change detection of the mangrove area in Hai Phong, Thai Binh and Nam Dinh provinces over 32 years. Overall, the mangrove area across the three provinces increased considerably since 2010. Hai Phong province had the largest area of mangrove in 2022 with 3934 ha, followed by Nam Dinh province (3591 ha). In contrast, the mangrove area in Thai Binh province was the lowest with 3195 ha.

Table 4. The change detection of the mangrove area in the three provinces over 32 years.

Year/Province	Hai Phong (ha)	Nam Dinh (ha)	Thai Binh (ha)	Total (ha)
1990	1433	459	1068	2960
1995	1190	776	442	2408
1990–1995	−243	317	−626	−552
2000	1495	1335	1605	4435
1995–2000	305	559	1163	2027
2005	1061	1287	1154	3502
2000–2005	−434	−48	−451	−933
2010	1628	1564	1514	4706
2005–2010	567	277	360	1204
2015	3065	2781	2333	8179
2010–2015	1437	1217	819	3473
2020	3790	3325	3010	10,125
2015–2020	725	544	677	1946
2022	3934	3591	3195	10,630
2020–2022	144	176	185	505

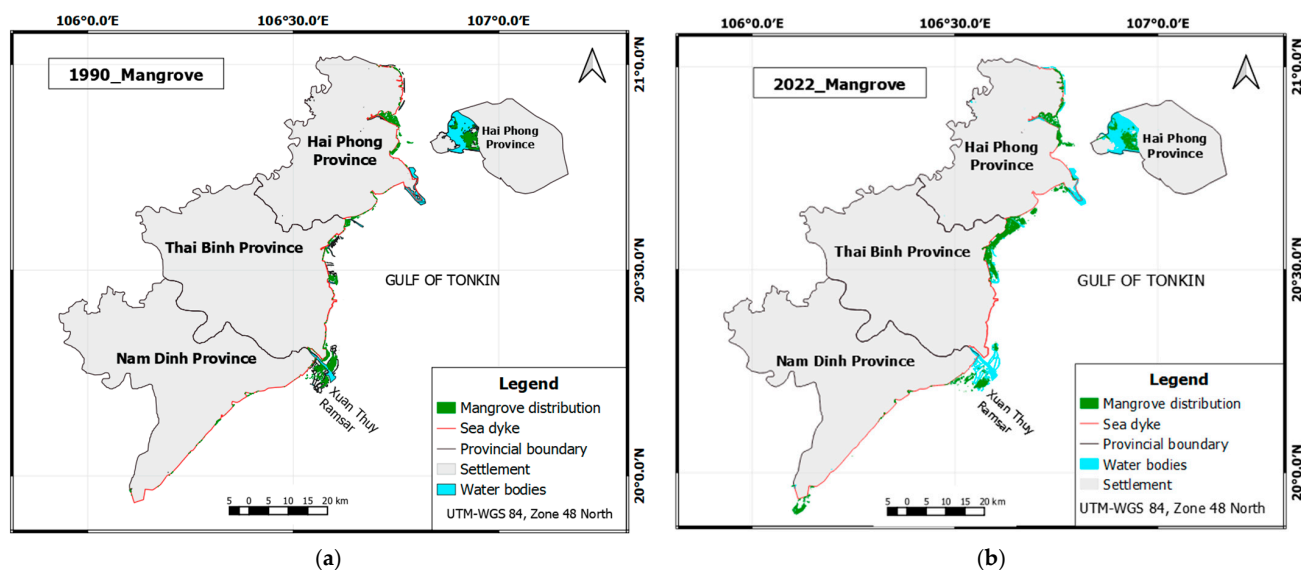


Figure 5. The spatial distribution map of mangrove in the RRD of Vietnam: (a) mangrove map in 1990; (b) mangrove map in 2022.

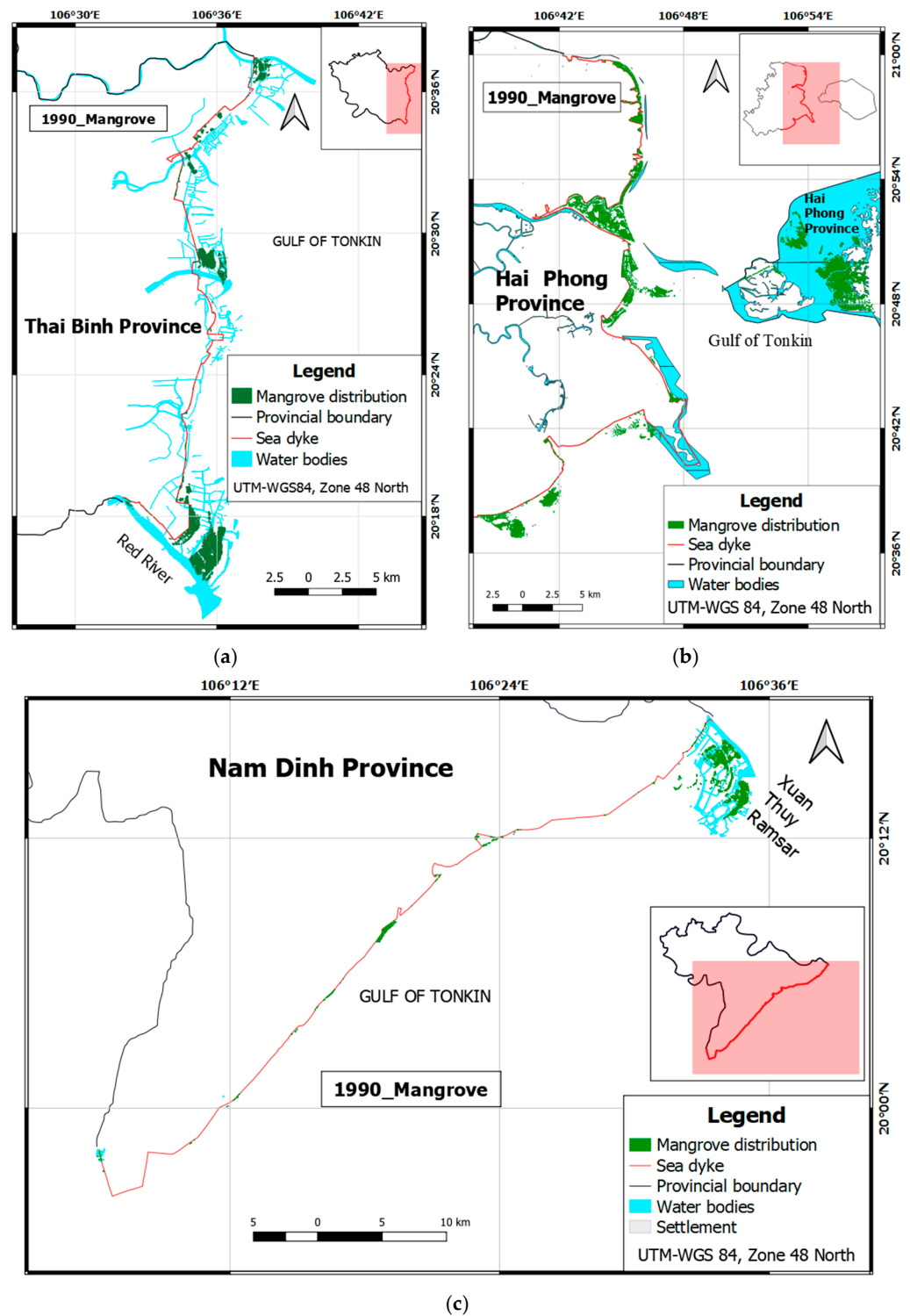


Figure 6. Mangrove maps in the three provinces in 1990 across the RRD, northern Vietnam: (a) Thai Binh; (b) Hai Phong; (c) Nam Dinh.

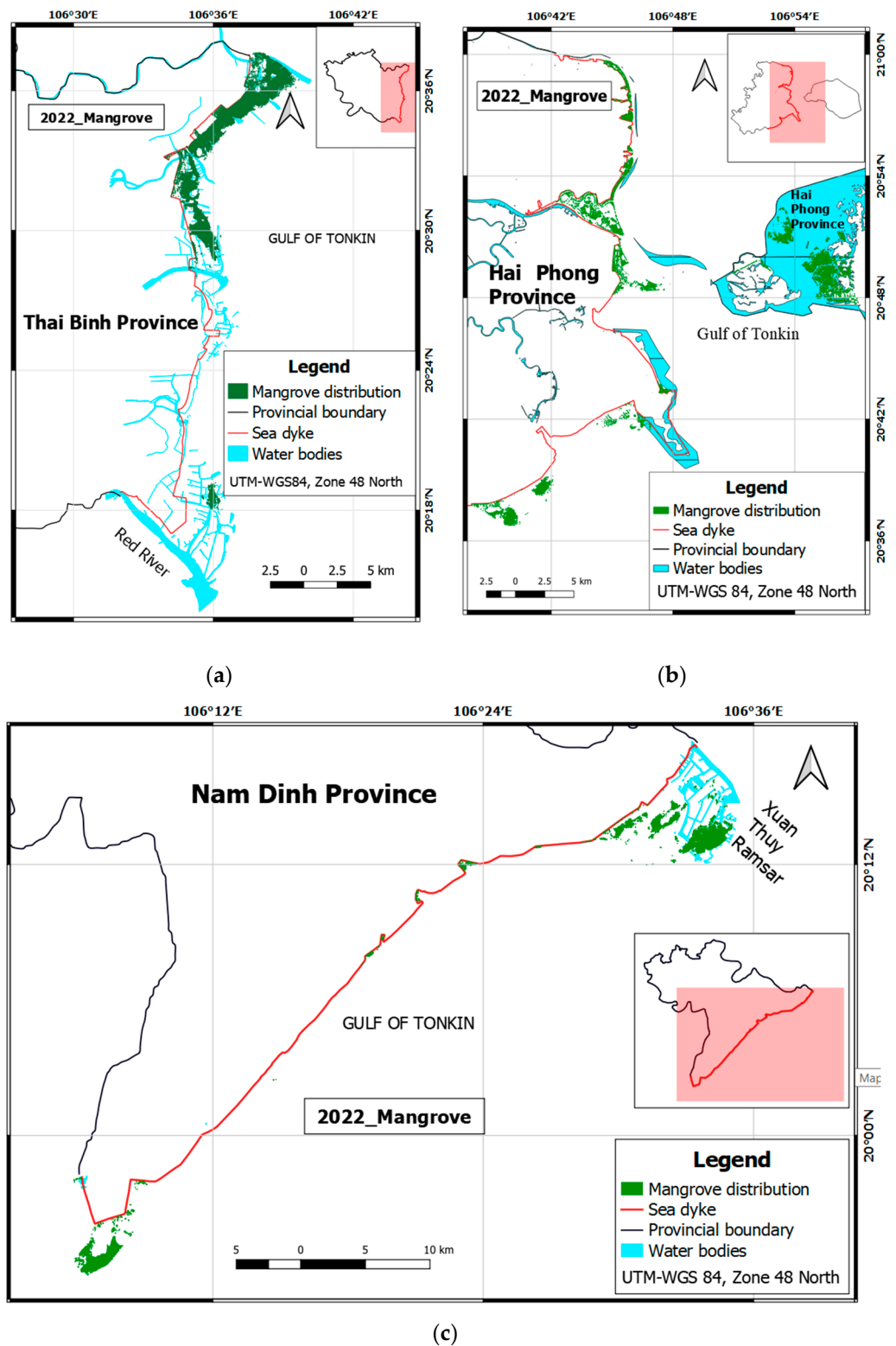


Figure 7. Mangrove maps in the three provinces in 2022 across the RRD, northern Vietnam: (a) Thai Binh; (b) Hai Phong; (c) Nam Dinh.

4. Discussion

4.1. Uncertainty of Mangrove Mapping and Change Detection

The overall accuracies (OA) of the mangrove maps in 2020 and in 2022 were 94.94% and 91.98% with Kappa coefficients of 0.90 and 0.84, respectively. These values indicate the successful use of the pixel-based algorithm for mapping mangrove forests and detecting change using multi-temporal Landsat datasets on the GEE cloud computing platform. The Landsat-8 OLI sensor produced better results than those obtained from Landsat-9 OLI-2 (Tables 2 and 3). It is likely due to more available multi-temporal Landsat-8 datasets in 2020 with 14 time series scenes compared to only 3 cloud-free scenes available during 2022. The number of available cloud-free time series Landsat data would influence the overall accuracy and produce better results when mapping mangrove forests using the pixel-based algorithm. Future studies applying our framework and thresholds should be further tested in other mangrove regions with more available Landsat-9 OLI-2. Our results suggested satisfactory accuracies for mapping mangrove forests during 2020 and 2022. These results are relatively higher than those reported by the previous studies in Vietnam using SPOT-7 imagery with a higher spatial resolution of 6 m (OA = 92.9%) [41] and using time series Landsat data (OA ranged from 85% to 92%) [42]. Our results are similar to Hauser et al. [43] with an attempt to detect mangrove dynamics on the southern coast of Vietnam using GEE with an overall accuracy ranging from 94 to 96%. However, there is an uncertainty involved in the mangrove classification and change detection. There are several factors that could affect the accuracy of mangrove mapping in the study area during 2020. As shown in Figure A4, this study only obtained about 83% of the pixels in 2020 with seven good-quality observations. Therefore, it can be considered that the acceptable uncertainty [40,41] in mangrove area estimation probably resulted from the lower quality of available Landsat time series (TM/ETM+/OLI/OLI-2) data obtained in the current study area between 1990 and 2022. In addition, the mixed pixels of mangrove and other vegetation in the study area may also affect the accuracy of the generated mangrove maps. For example, *Casuarina* spp. sites were misclassified as mangrove forests because several *Casuarina* spp. species have a quite similar reflectance spectrum with other mangrove species observed in the RRD [30] such as *Sonneratia caseolaris*, *Kandelia obovata*, *Aegiceras corniculatum*, *Rhizophora stylosa* and *Avicennia marina*. Importantly, in the RRD, many mixed small and shrub species are often observed and reported in the previous studies [30,35].

In this study, the defined thresholds were created based on the calibration data collected from the high spatial resolution Google Earth images in 2020 to automatically map and detect mangrove canopy changes across the RRD. As shown in Figure 4, the estimated mangrove area in 2015 was about 8179 ha. This number is close to the estimate as reported in the National Forest Inventory (NFI) in Vietnam during 2015 (8225 ha), fitting well with the model developed in the current study using Landsat data on the GEE.

We observed an increase in the extent of mangroves across the three provinces in the RRD located on the northern coast of Vietnam from 1990 to 2022. The trend is consistent with the forest coverage change in Vietnam, which was reported in recent studies [44,45] and is similar to those observed in other Southeast Asian countries by Goldberg et al. [3] in the southeast and northern Australia by Saintilan et al. [4]. The increase in forest coverage benefited from the efforts of the Vietnamese government in mangrove planting, restoration, and protection. The total forest area in Vietnam was slightly increased between 1990 and 2020 and includes both inland forest and mangrove forest in Vietnam [44]. Overall, the mangrove forest area increase over 32 years (1990–2022) can be automatically detected and mapped by using Landsat 5/7/8/9 time series images through the GEE platform as a result of a number of mangrove restoration projects and programs by the Vietnamese government and policy recommendations based on policy measures from many research studies [11,46].

4.2. Driving Factors for Mangrove Dynamic in Three Provinces from 1990 to 2022

As exhibited in Table 4 and Figure 4, the mangrove area changed during the period of 1990–2022. Key drivers that caused changes of mangrove forests in each period are considered and discussed as follows:

Between 1990 and 1995: The total mangrove area of three provinces decreased from 2960 ha in 1990 to 2408 ha in 1995. This decline was caused by the mangrove deforestation in the Hai Phong province and the Thai Binh province during the period. Specifically, the mangrove area in Hai Phong province declined from 1433 ha to 1190 ha, and in Thai Binh province it reduced from 1068 ha to 442 ha. This period witnessed the smallest mangrove area during the 32-year period. The reasons behind the decrease were the consequence of a new policy, the Reform Policy, initiated in 1986 and officially launched in 1991 [47]. During the period, natural resources, including forest resources, were exhaustively exploited for economic development.

During this period, many regions were converted to aquaculture farms, significantly destroying mangrove forests in Thai Binh and Hai Phong provinces [10]. In contrast, Nam Dinh province had a mangrove area increase of 317 ha from 1990 to 1995 thanks to strict protection and constant expansion of Xuan Thuy National Park [48].

Period of 1995–2000: This period witnessed an increase in the mangrove area in three provinces (Table 4). The mangrove areas of Hai Phong, Nam Dinh and Thai Binh provinces in 2000 reached 1495 ha, 1335 ha and 1605 ha, respectively. This increase was due mainly to the efforts of planting and protecting mangrove forests through various programs and projects implemented in such provinces. During this period, the Five Million Hectare Reforestation Program (661 program) was carried out between 1998 and 2010 at the national level to increase forest coverage. The percentage of forest coverage was up to 43% of the total land cover in the final year of the program. In addition, other programs and projects were also implemented. Several projects such as Red Cross of Japan, PAM5325, ACTMANG, the 661 programs (Mangrove Plantation and Disaster Risk Reduction project) were undertaken in such provinces. These projects significantly contributed to the increase of mangrove cover in the RRD [49,50].

Period of 2000–2005: In this period, the mangrove areas decreased from 4435 ha in 2000 to 3502 ha in 2005 (Figure 4). The main cause for mangrove loss in 2005 may probably be explained by the negative impacts of natural disasters. In 2005, an extreme typhoon event, typhoon “Damrey”, hit the northern region of Vietnam [46] and damaged the mangrove forest in these areas, especially young mangrove forests. This typhoon was also reported by Hong, Avtar and Fujii [9] as the amongst the strongest tropical cyclones impacting the coastal zones of Vietnam during the last 30 years.

Period 2005–2020: This period witnessed a continuous increase in the area of mangroves in such provinces sustained for 15 years. As shown in Table 4, the total area of mangrove reached 10,125 ha in 2020. This number was three-times higher than that in 2005. The mangrove restoration received priority attention and investment by the Vietnamese government in this period and enhancement of community-based mangrove management [51,52]. In addition to the 661 Program implemented from 1998 to 2010, many other projects and programs funded by the Vietnamese government and other organizations were implemented in the whole country [52], especially in the Red River Delta [53]. Further sustainable mangrove conservation and management across the Vietnamese coastline should be carefully considered in protecting existed mangrove forests and restoring degraded mangroves as well as planting new ones to enhance not only the mangrove area but also quality and biodiversity in the context of climate change issues.

Period 2020–2022: This short period was characterised by an increased upward trend in mangrove area in the RRD. The Vietnamese government continued to support mangrove conservation and management schemes in dealing with climate change impact.

5. Conclusions

Mangrove forests play an important role in mitigating climate change impacts and are able to sequester blue carbon for their protection and restoration. Mapping mangrove extent at a large scale remains challenging due to cloud coverage and spatial limitations of single satellite sensors. This study developed a framework using the pixel-based algorithm applied to Landsat TM/ETM+/OLI/OLI-2 time series data on the Google Earth Engine cloud computing platform to automatically map and quantify mangrove forest changes in the three provinces of Hai Phong, Nam Dinh and Thai Binh across the RRD over 32 years.

The results showed that the mangrove area has increased considerably in the RRD over 32 years in response to the mangrove restoration programs and policies by the Vietnamese government and local governments. The mangrove areas were 2960 ha, 2408 ha, 4435 ha, 3502 ha, 4706 ha, 8179 ha, 10,125 ha and 10,630 ha in 1990, 1995, 2000, 2005, 2010, 2015, 2020 and 2022, respectively.

The overall accuracies of the Landsat-8 OLI and the Landsat-9 OLI-2 image processing for 2020 and 2022 were 94.94% and 91.98%, respectively, while the Kappa coefficients were 0.90 and 0.84, indicating promising results for mapping mangrove forest cover in the tropics using the GEE platform associated with free open-source code. It could be said that the pixel-based algorithm and Landsat time series images on the GEE cloud computing are suitable for long-term monitoring of mangrove change in tropical regions. The Landsat family has shown the potential use in mapping mangrove dynamics in the tropics and should be further used worldwide.

Author Contributions: Conceptualization, T.T.P.V., T.D.P. and B.M.; methodology, T.T.P.V., T.D.P., H.V.L. and Q.H.V.; software, T.T.P.V. and H.Q.N.; validation, T.T.P.V., Q.H.V. and T.D.P.; formal analysis, T.T.P.V. and H.Q.N.; investigation, T.T.P.V.; resources, T.T.P.V. and N.N.L.; data curation, T.T.P.V.; writing—original draft preparation, T.T.P.V. and T.D.P.; writing—review and editing, T.D.P., N.S., N.N.L. and A.S.; visualization, T.D.P. and H.V.L.; supervision, B.M. All authors have read and agreed to the published version of the manuscript.

Funding: This research received no external funding.

Data Availability Statement: Not applicable.

Acknowledgments: The authors are thankful to the JICE (Japanese International Cooperation Center) for financial support to the first author studying a master course at the University of Tsukuba, Japan for 2 years. In addition, we also would like to thank the Forest Inventory and Planning Institute (FIPI), Vietnam for providing useful data for the current study. T.D.P. is supported by a Macquarie University Research Fellowship (Grant No. MQRF0001124-2021).

Conflicts of Interest: The authors declare no conflict of interest.

Appendix A

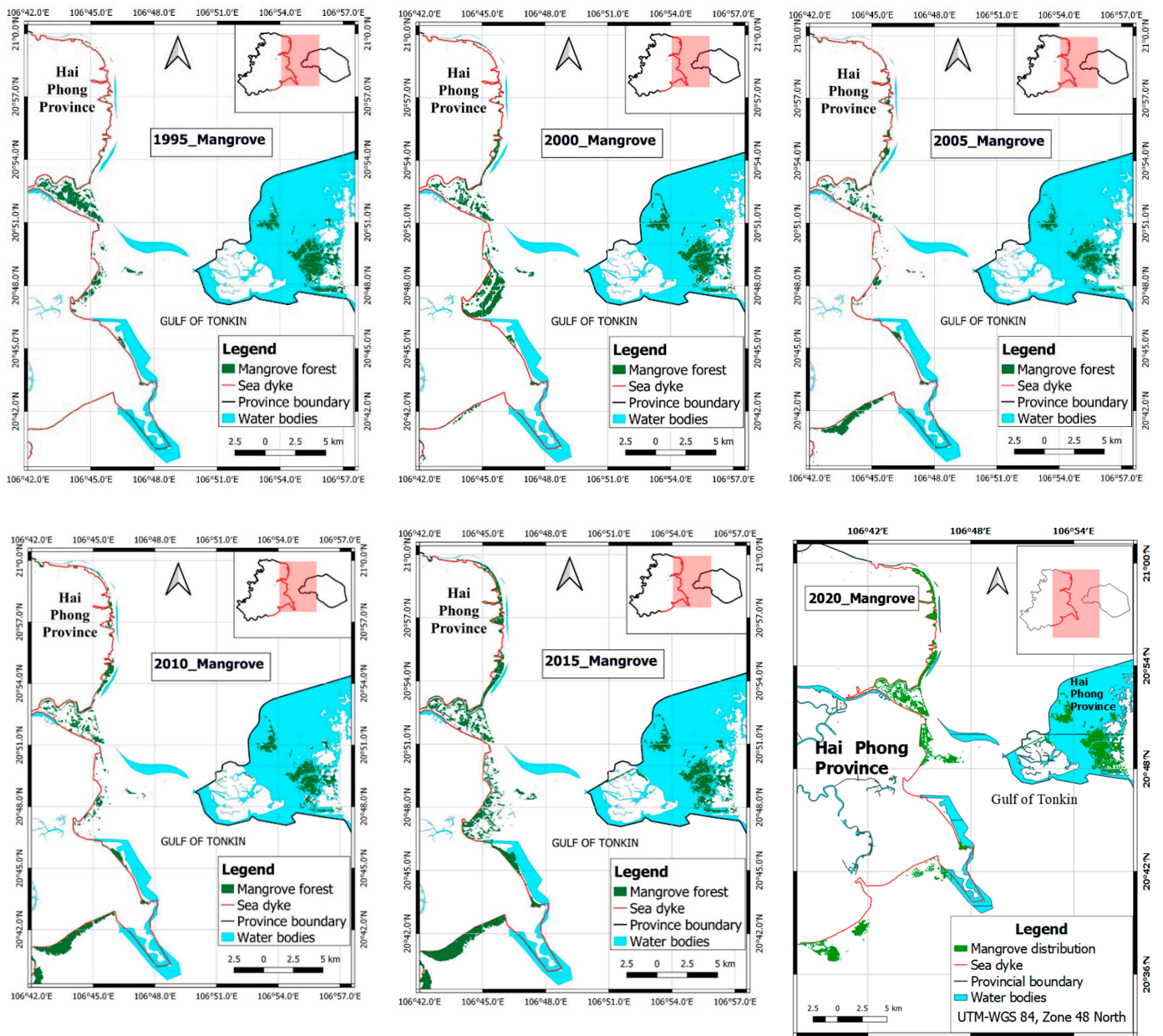


Figure A1. Mangrove distribution maps in Hai Phong between 1995 and 2020.

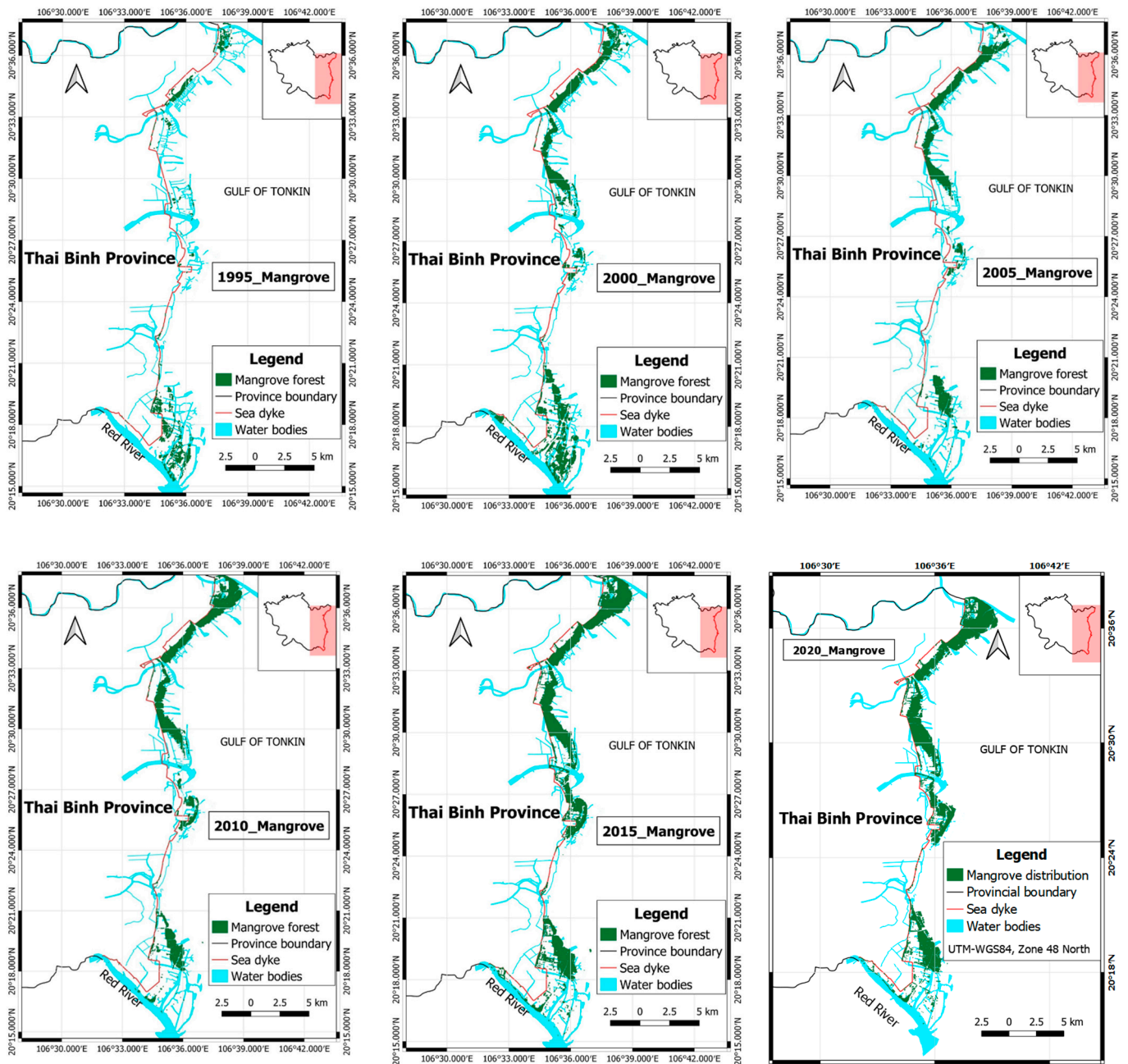


Figure A2. Mangrove distribution maps in Thai Binh between 1995 and 2020.

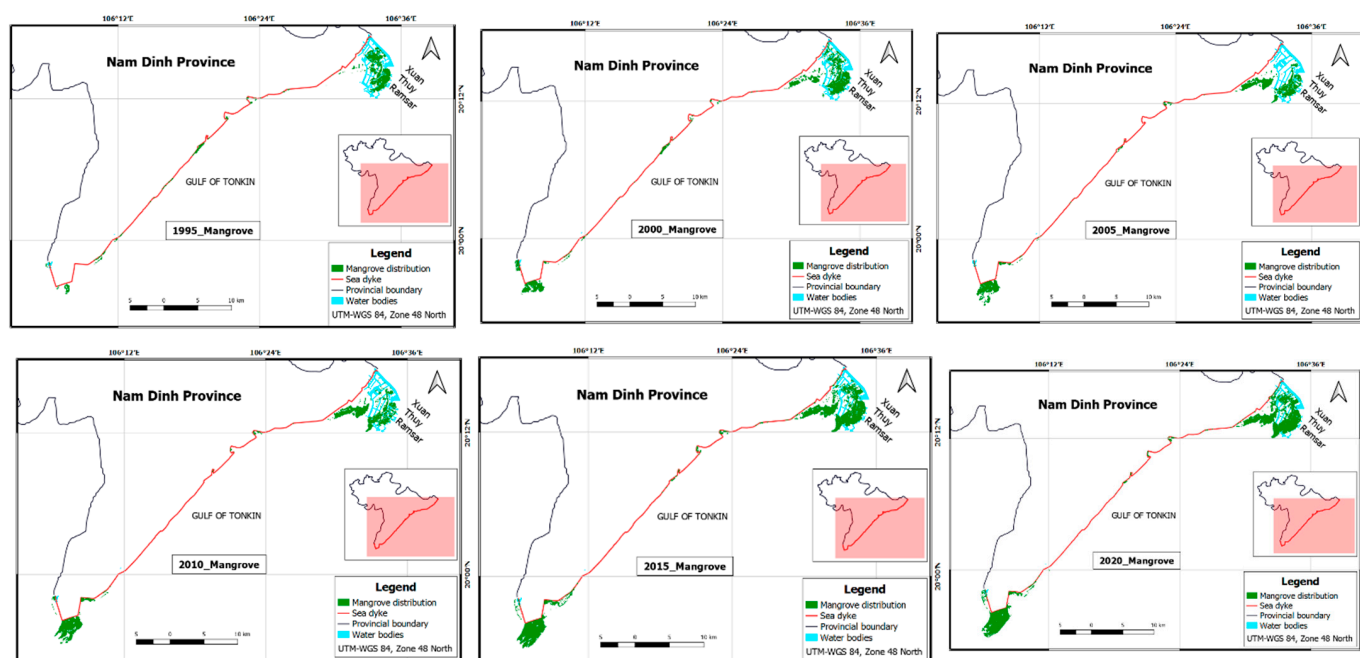


Figure A3. Mangrove distribution maps in Nam Dinh between 1995 and 2020.

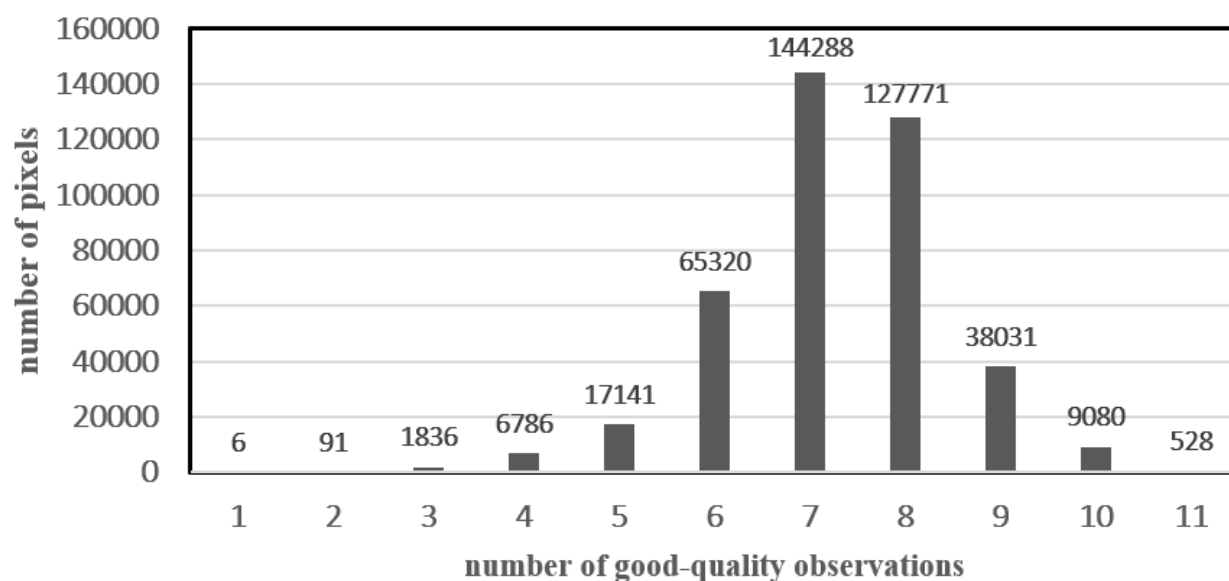


Figure A4. The number of pixels with good-quality observations in 2020.

References

1. Saintilan, N.; Khan, N.S.; Ashe, E.; Kelleway, J.J.; Rogers, K.; Woodroffe, C.D.; Horton, B.P. Thresholds of mangrove survival under rapid sea level rise. *Science* **2020**, *368*, 1118. [[CrossRef](#)] [[PubMed](#)]
2. Friess, D.A.; Rogers, K.; Lovelock, C.E.; Krauss, K.W.; Hamilton, S.E.; Lee, S.Y.; Lucas, R.; Primavera, J.; Rajkaran, A.; Shi, S. The State of the World's Mangrove Forests: Past, Present, and Future. *Annu. Rev. Environ. Resour.* **2019**, *44*, 89–115. [[CrossRef](#)]
3. Goldberg, L.; Lagomasino, D.; Thomas, N.; Fatoyinbo, T. Global declines in human-driven mangrove loss. *Glob. Change Biol.* **2020**, *26*, 5844–5855. [[CrossRef](#)] [[PubMed](#)]
4. Saintilan, N.; Asbridge, E.; Lucas, R.; Rogers, K.; Wen, L.; Powell, M.; Colloff, M.J.; Rodriguez, J.F.; Saco, P.M.; Sandi, S.; et al. Australian forested wetlands under climate change: Collapse or proliferation? *Mar. Freshw. Res.* **2021**, *73*, 1255–1262. [[CrossRef](#)]
5. Saintilan, N.; Wilson, N.C.; Rogers, K.; Rajkaran, A.; Krauss, K.W. Mangrove expansion and salt marsh decline at mangrove poleward limits. *Glob. Change Biol.* **2014**, *20*, 147–157. [[CrossRef](#)]
6. Hong, P.N.; San, H.T. *Mangroves of Vietnam*; IUCN: Bangkok, Thailand, 1993; p. 173.
7. Warner, R.; Kaidonis, M.; Dun, O.; Rogers, K.; Shi, Y.; Nguyen, T.T.X.; Woodroffe, C.D. Opportunities and challenges for mangrove carbon sequestration in the Mekong River Delta in Vietnam. *Sustain. Sci.* **2016**, *11*, 661–677. [[CrossRef](#)]

8. Veettil, B.K.; Ward, R.D.; Quang, N.X.; Trang, N.T.T.; Giang, T.H. Mangroves of Vietnam: Historical development, current state of research and future threats. *Estuar. Coast. Shelf Sci.* **2019**, *218*, 212–236. [[CrossRef](#)]
9. Hong, H.T.C.; Avtar, R.; Fujii, M. Monitoring changes in land use and distribution of mangroves in the southeastern part of the Mekong River Delta, Vietnam. *Trop. Ecol.* **2019**, *60*, 552–565. [[CrossRef](#)]
10. Pham, T.D.; Yoshino, K. Mangrove Mapping and Change Detection Using Multi-temporal Landsat imagery in Hai Phong city, Vietnam. In Proceedings of the International Symposium on Cartography in Internet and Ubiquitous Environments 2015, Tokyo, Japan, 17–19 March 2015.
11. Tran, L.X.; Fischer, A. Spatiotemporal changes and fragmentation of mangroves and its effects on fish diversity in Ca Mau Province (Vietnam). *J. Coast. Conserv.* **2017**, *21*, 355–368. [[CrossRef](#)]
12. Nguyen-Thanh, S.; Chen, C.-F.; Chang, N.-B.; Chen, C.-R.; Chang, L.-Y.; Bui, X.-T. Mangrove Mapping and Change Detection in Ca Mau Peninsula, Vietnam, Using Landsat Data and Object-Based Image Analysis. *IEEE J. Sel. Top. Appl. Earth Obs. Remote Sens.* **2015**, *8*, 503–510. [[CrossRef](#)]
13. Pham, L.T.H.; Brabyn, L. Monitoring mangrove biomass change in Vietnam using SPOT images and an object-based approach combined with machine learning algorithms. *ISPRS J. Photogramm. Remote Sens.* **2017**, *128*, 86–97. [[CrossRef](#)]
14. Pham, T.D.; Yoshino, K. Monitoring Mangrove Forest using Multi-temporal Satellite Data in the Northern Coast of Vietnam. In Proceedings of the 32nd Asian Conference on Remote Sensing, Taipei, Taiwan, 3–7 October 2011.
15. Lymburner, L.; Bunting, P.; Lucas, R.; Scarth, P.; Alam, I.; Phillips, C.; Ticehurst, C.; Held, A. Mapping the multi-decadal mangrove dynamics of the Australian coastline. *Remote Sens. Environ.* **2020**, *238*, 111185. [[CrossRef](#)]
16. Long, J.B.; Giri, C. Mapping the Philippines' Mangrove Forests Using Landsat Imagery. *Sensors* **2011**, *11*, 2972–2981. [[CrossRef](#)]
17. Giri, C.; Ochieng, E.; Tieszen, L.L.; Zhu, Z.; Shingh, A.; Loveland, T. Status and distribution of mangrove forests of the world using earth observation satellite data. *Glob. Ecol. Biogeogr.* **2011**, *20*, 154–159. [[CrossRef](#)]
18. Giri, C.; Pengra, B.; Zhu, Z.; Singh, A.; Tieszen, A.L.L. Monitoring mangrove forest dynamics of the Sundarbans in Bangladesh and India using multi-temporal satellite data from 1973 to 2000. *Estuar. Coast. Shelf Sci.* **2007**, *73*, 91–100. [[CrossRef](#)]
19. Pham, T.D.; Yokoya, N.; Bui, D.T.; Yoshino, K.; Friess, D.A. Remote Sensing Approaches for Monitoring Mangrove Species, Structure, and Biomass: Opportunities and Challenges. *Remote Sens.* **2019**, *11*, 230. [[CrossRef](#)]
20. Pham, T.D.; Xia, J.; Ha, N.T.; Bui, D.T.; Le, N.N.; Takeuchi, W. A Review of Remote Sensing Approaches for Monitoring Blue Carbon Ecosystems: Mangroves, Seagrasses and Salt Marshes during 2010–2018. *Sensors* **2019**, *19*, 1933. [[CrossRef](#)]
21. Yancho, J.M.M.; Jones, T.G.; Gandhi, S.R.; Ferster, C.; Lin, A.; Glass, L. The Google Earth Engine Mangrove Mapping Methodology (GEEMMM). *Remote Sens.* **2020**, *12*, 3758. [[CrossRef](#)]
22. Wang, X.; Xiao, X.; Zou, Z.; Hou, L.; Qin, Y.; Dong, J.; Doughty, R.B.; Chen, B.; Zhang, X.; Chen, Y.; et al. Mapping coastal wetlands of China using time series Landsat images in 2018 and Google Earth Engine. *ISPRS J. Photogramm. Remote Sens.* **2020**, *163*, 312–326. [[CrossRef](#)]
23. Mahdianpari, M.; Brisco, B.; Granger, J.E.; Mohammadimanesh, F.; Salehi, B.; Banks, S.; Homayouni, S.; Bourgeau-Chavez, L.; Weng, Q. The Second Generation Canadian Wetland Inventory Map at 10 Meters Resolution Using Google Earth Engine. *Can. J. Remote Sens.* **2020**, *46*, 360–375. [[CrossRef](#)]
24. Chen, B.; Xiao, X.; Li, X.; Pan, L.; Doughty, R.; Ma, J.; Dong, J.; Qin, Y.; Zhao, B.; Wu, Z.; et al. A mangrove forest map of China in 2015: Analysis of time series Landsat 7/8 and Sentinel-1A imagery in Google Earth Engine cloud computing platform. *ISPRS J. Photogramm. Remote Sens.* **2017**, *131*, 104–120. [[CrossRef](#)]
25. Masek, J.G.; Wulder, M.A.; Markham, B.; McCorkel, J.; Crawford, C.J.; Storey, J.; Jenstrom, D.T. Landsat 9: Empowering open science and applications through continuity. *Remote Sens. Environ.* **2020**, *248*, 111968. [[CrossRef](#)]
26. Pham, T.D.; Yokoya, N.; Nguyen, T.T.T.; Le, N.N.; Ha, N.T.; Xia, J.; Takeuchi, W.; Pham, T.D. Improvement of Mangrove Soil Carbon Stocks Estimation in North Vietnam Using Sentinel-2 Data and Machine Learning Approach. *GISci. Remote Sens.* **2021**, *58*, 68–87. [[CrossRef](#)]
27. Pham, T.D.; Yokoya, N.; Xia, J.; Ha, N.T.; Le, N.N.; Nguyen, T.T.T.; Dao, T.H.; Vu, T.T.P.; Pham, T.D.; Takeuchi, W. Comparison of Machine Learning Methods for Estimating Mangrove Above-Ground Biomass Using Multiple Source Remote Sensing Data in the Red River Delta Biosphere Reserve, Vietnam. *Remote Sens.* **2020**, *12*, 1334. [[CrossRef](#)]
28. Seto, K.C.; Fragkias, M. Mangrove conversion and aquaculture development in Vietnam: A remote sensing-based approach for evaluating the Ramsar Convention on Wetlands. *Glob. Environ. Change* **2007**, *17*, 486–500. [[CrossRef](#)]
29. Halls, A. *Wetlands, Biodiversity and the Ramsar Convention: The Role of the Convention on Wetlands in the Conservation and Wise Use of Biodiversity*; Ramsar Convention Bureau: Gland, Switzerland, 1997.
30. Xia, J.; Yokoya, N.; Pham, T.D. Probabilistic Mangrove Species Mapping with Multiple-Source Remote-Sensing Datasets Using Label Distribution Learning in Xuan Thuy National Park, Vietnam. *Remote Sens.* **2020**, *12*, 3834. [[CrossRef](#)]
31. Mai, C.V.; Stive, M.J.F.; Gelder, P.H. Coastal Protection Strategies for the Red River Delta. *J. Coast. Res.* **2009**, *25*, 105–116. [[CrossRef](#)]
32. Quartel, S.; Kroon, A.; Augustinus, P.G.E.F.; Van Santen, P.; Tri, N.H. Wave attenuation in coastal mangroves in the Red River Delta, Vietnam. *J. Asian Earth Sci.* **2007**, *29*, 576–584. [[CrossRef](#)]
33. Thomas, N.; Bunting, P.; Lucas, R.; Hardy, A.; Rosenqvist, A.; Fatoyinbo, T. Mapping Mangrove Extent and Change: A Globally Applicable Approach. *Remote Sens.* **2018**, *10*, 1466. [[CrossRef](#)]

34. Bunting, P.; Rosenqvist, A.; Hilarides, L.; Lucas, R.M.; Thomas, N. Global Mangrove Watch: Updated 2010 Mangrove Forest Extent (v2.5). *Remote Sens.* **2022**, *14*, 1034. [[CrossRef](#)]
35. Pham, T.D.; Xia, J.; Baier, G.; Le, N.N.; Yokoya, N. Mangrove Species Mapping Using Sentinel-1 and Sentinel-2 Data in North Vietnam. In Proceedings of IGARSS 2019—2019 IEEE International Geoscience and Remote Sensing Symposium, Yokohama, Japan, 28 July–2 August 2019; pp. 6102–6105.
36. Rouse, J.W., Jr.; Haas, R.; Schell, J.; Deering, D. *Monitoring Vegetation Systems in the Great Plains with ERTS*; NASA Special Publication: Washington, DC, USA, 1974.
37. Liu, H.Q.; Huete, A. A feedback based modification of the NDVI to minimize canopy background and atmospheric noise. *IEEE Trans. Geosci. Remote Sens.* **1995**, *33*, 457–465. [[CrossRef](#)]
38. Xiao, X.; Boles, S.; Liu, J.; Zhuang, D.; Liu, M. Characterization of forest types in Northeastern China, using multi-temporal SPOT-4 VEGETATION sensor data. *Remote Sens. Environ.* **2002**, *82*, 335–348. [[CrossRef](#)]
39. Xu, H. Modification of normalised difference water index (NDWI) to enhance open water features in remotely sensed imagery. *Int. J. Remote Sens.* **2006**, *27*, 3025–3033. [[CrossRef](#)]
40. Ha, N.T.; Manley-Harris, M.; Pham, T.D.; Hawes, I. A Comparative Assessment of Ensemble-Based Machine Learning and Maximum Likelihood Methods for Mapping Seagrass Using Sentinel-2 Imagery in Tauranga Harbor, New Zealand. *Remote Sens.* **2020**, *12*, 355. [[CrossRef](#)]
41. Quang, N.H.; Quinn, C.H.; Stringer, L.C.; Carrie, R.; Hackney, C.R.; Van Hue, L.T.; Van Tan, D.; Nga, P.T.T. Multi-Decadal Changes in Mangrove Extent, Age and Species in the Red River Estuaries of Viet Nam. *Remote Sens.* **2020**, *12*, 2289. [[CrossRef](#)]
42. Nguyen, H.-H.; Tran, L.T.N.; Le, A.T.; Nghia, N.H.; Duong, L.V.K.; Nguyen, H.T.T.; Bohm, S.; Premnath, C.F.S. Monitoring Changes in Coastal Mangrove Extents Using Multi-Temporal Satellite Data in Selected Communes, Hai Phong City, Vietnam. *For. Soc.* **2020**, *4*, 256–270. [[CrossRef](#)]
43. Hauser, L.T.; An Binh, N.; Viet Hoa, P.; Hong Quan, N.; Timmermans, J. Gap-Free Monitoring of Annual Mangrove Forest Dynamics in Ca Mau Province, Vietnamese Mekong Delta, Using the Landsat-7-8 Archives and Post-Classification Temporal Optimization. *Remote Sens.* **2020**, *12*, 3729. [[CrossRef](#)]
44. Phan, D.C.; Trung, T.H.; Truong, V.T.; Sasagawa, T.; Vu, T.P.T.; Bui, D.T.; Hayashi, M.; Tadono, T.; Nasahara, K.N. First comprehensive quantification of annual land use/cover from 1990 to 2020 across mainland Vietnam. *Sci. Rep.* **2021**, *11*, 9979. [[CrossRef](#)]
45. Truong, V.T.; Hoang, T.T.; Cao, D.P.; Hayashi, M.; Tadono, T.; Nasahara, K.N. JAXA Annual Forest Cover Maps for Vietnam during 2015–2018 Using ALOS-2/PALSAR-2 and Auxiliary Data. *Remote Sens.* **2019**, *11*, 2412. [[CrossRef](#)]
46. Pham, T.D.; Yoshino, K. Impacts of mangrove management systems on mangrove changes in the Northern Coast of Vietnam. *Tropics* **2016**, *24*, 141–151. [[CrossRef](#)]
47. Phuong, N.C.; Richard, J. Economic Transition and Accounting System Reform in Vietnam. *Eur. Account. Rev.* **2011**, *20*, 693–725. [[CrossRef](#)]
48. Leslie, M.; Nguyen, S.T.; Nguyen, T.K.D.; Pham, T.T.; Cao, T.T.N.; Le, T.Q.; Dang, T.T.; Nguyen, T.H.T.; Nguyen, T.B.N.; Le, H.N.; et al. Bringing social and cultural considerations into environmental management for vulnerable coastal communities: Responses to environmental change in Xuan Thuy National Park, Nam Dinh Province, Vietnam. *Ocean. Coast. Manag.* **2018**, *158*, 32–44. [[CrossRef](#)]
49. Hai, N.T.; Dell, B.; Phuong, V.T.; Harper, R.J. Towards a more robust approach for the restoration of mangroves in Vietnam. *Ann. For. Sci.* **2020**, *77*, 18. [[CrossRef](#)]
50. Nguyen, H.T.; Yoneda, R.; Ninomiya, I.; Harada, K.; Dao, T.V.; Sy, T.M.; Phan, H.N. The effects of stand-age and inundation on carbon accumulation in mangrove plantation soil in Namdinh, Northern Vietnam. *Tropics* **2004**, *14*, 21–37. [[CrossRef](#)]
51. Powell, N.; Osbeck, M.; Tan, S.B.; Toan, V.C. Mangrove restoration and rehabilitation for climate change adaptation in Vietnam. In *World Resources Report Case Study*; World Resources Report; World Resources: Washington, DC, USA, 2011. Available online: <http://www.worldresourcesreport.org> (accessed on 25 November 2021).
52. Nguyen, T.P.; Van Tam, N.; Quoi, L.P.; Parnell, K.E. Community perspectives on an internationally funded mangrove restoration project: Kien Giang province, Vietnam. *Ocean. Coast. Manag.* **2016**, *119*, 146–154. [[CrossRef](#)]
53. Pham, T.T.; Vu, T.P.; Hoang, T.L.; Dao, T.L.C.; Nguyen, D.T.; Pham, D.C.; Dao, L.H.T.; Nguyen, V.T.; Hoang, N.V.H. The Effectiveness of Financial Incentives for Addressing Mangrove Loss in Northern Vietnam. *Front. For. Glob. Change* **2022**, *4*, 709073. [[CrossRef](#)]